Alternating Gradient Synchrotron Department
Relativistic Heavy Ion Collider Project
BROOKHAVEN NATIONAL LABORATORY
Upton, New York 11973

Spin Note

AGS/RHIC/SN No. 046

Multipole Components in the BNL Type Helical Dipole Magnet

M. Okamura

November 12, 1996

For Internal Distribution Only

Multipole Components in the BNL Type Helical Dipole Magnet

M. Okamura

Abstract

Using three dimensional (3D) magnetic field calculation code TOSCA, Multipole components in the BNL type Helical Dipole Magnet were analyzed. The effects of the helical structure to the multipole component were also investigated.

1. Introduction

The expected multipole components in the helical dipole magnet which is being fabricated in BNL were analyzed by TOSCA and OPERA. In this magnet design, to optimize multipole components, two dimensional (2D) calculation using POISSON has been done. Actually, there are longitudinal magnetic fields in the helical magnets and 2D methods seem insufficient to design highly uniformed magnets. So, 3D analysis is required to study the effect of the helical structure on the multipole components. Similarly, the effect of slight difference between the design cross section and the actual coil position was checked.

2. Magnetic calculation about straight coil using TOSCA

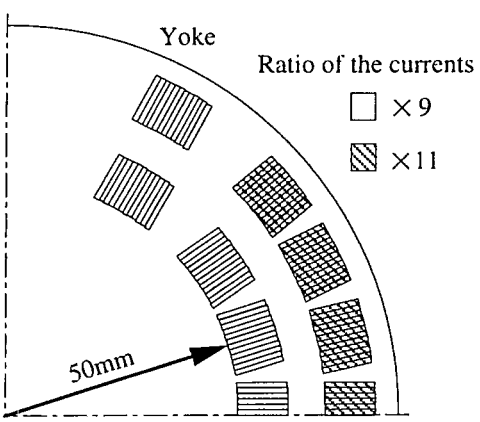

Fig. 1 Optimized cross section of the Snake Magnet

At first, before describing results of the 3D calculations about the helical structure, a comparison of magnetic field optimized by POISSON and the field calculated using TOSCA is described. Figure 1 shows a cross sectional view of the Snake Magnet optimized[1] using POISSON. Each rectangle consists of 9 layered cables, and the total of 12 rectangles fit in a slot. As indicated in Fig. 1, two levels of currents are applied in the ratio of 9 to 11. To confirm the reliability of calculation by TOSCA, a field in untwisted conductors, straight bar, which has completely same shape as shown at Fig. 1 was analyzed using

TOSCA. In this analysis, the shape of the yoke and mesh size are almost same that will be used in the calculation of the Helical Dipole Magnets described later in this note. The calculated multipole components along the circle of 3.0 cm radius at the center of the magnet are shown in Table 1. The current used in Low current analysis is a just one-tenth of the High current case. In low current calculation, there is not an effect of magnetic saturation of iron yoke and this is the same condition which has been used in the optimization by using POISSON. The calculated sextupole and decapole components using TOSCA are small enough, and agree with the result of POISSON.

Table 1 Multipole coefficients in the straight coil calculated by TOSCA.

		Low current	High current
Reference radius	cm	3.0	3.0
Dipole component	Gauss	4380	40570
Sextupole component	Gauss	0.934	113
Decapole component	Gauss	0.253	8.80
Ratio of Sext. comp.	%	0.0213	0.279
Ratio of Deca. comp.	%	0.00578	0.0217

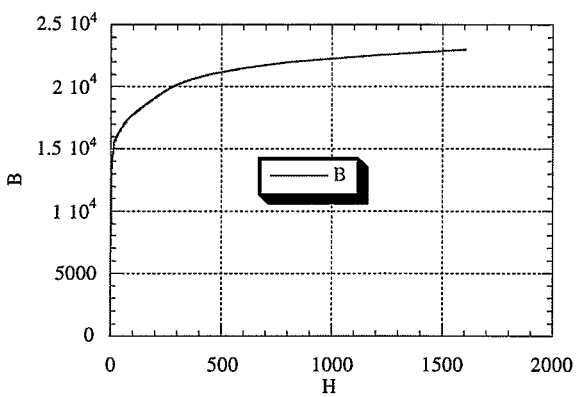

Fig. 2 BH curve

In the case of High current, the predicted ratios of multipole component become large due to the iron saturation, however, according to R. Gupta, the multipole components can be controlled by changing the ratio of electric currents which is now 9 to 11. A saturation characteristic of the iron of the yoke used for this magnetic field calculation are shown in Fig. 2. The specific permeability used in small strength region is 6400 Gauss/Oersted.

3. 3D calculation without yoke

OPERA, which is pre and post processor for TOSCA, can analyze magnetic fields without the effect of the yoke omitting time consuming finite element calculation. Using this code, three types of coils without yokes were analyzed. The first coil, Type 1 shown in Fig. 3, is made on the basis of the cross section designed by the 2D calculation considered in Section 2. The third, Type 3 coil shown in Fig. 5, was made using end data created by G. Morgan and corresponds to the coil of a full length Snake Magnet based on the half length

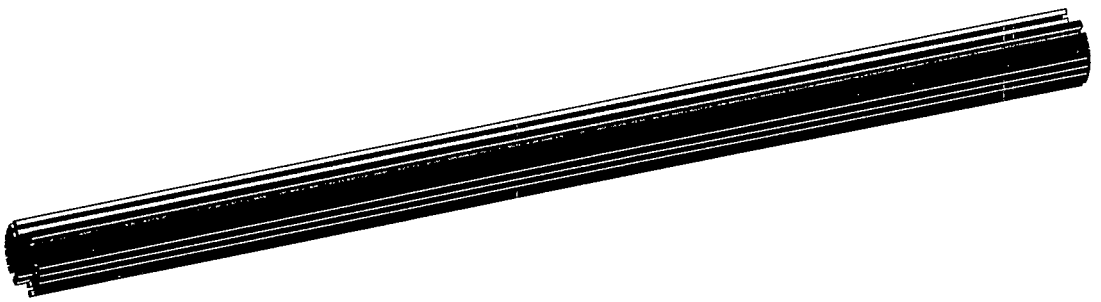

Fig. 3 Type 1, straight bars

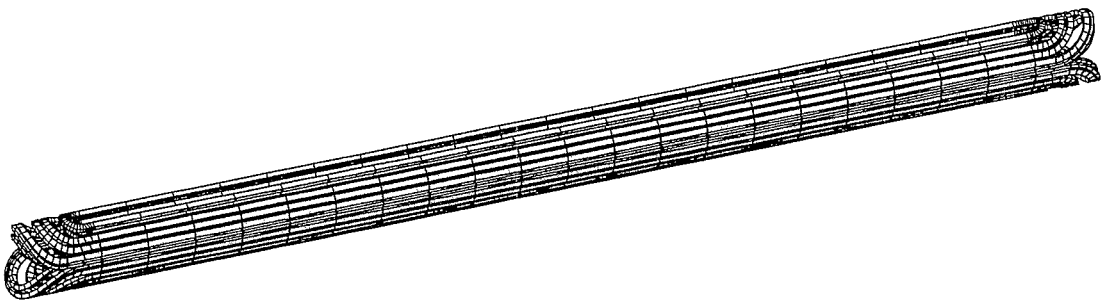

Fig. 4 Type 2, straightened helical coils

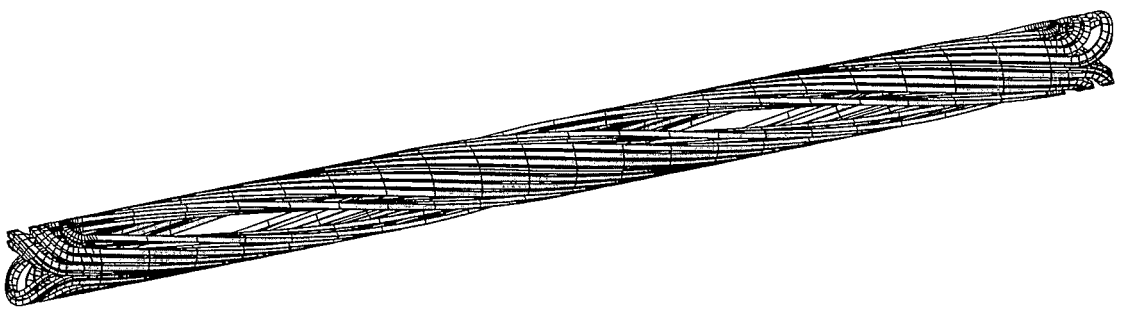

Fig. 5 Type 3, helical coils

model which is now being fabricated at BNL. The height of each conductor was set to be 10.36 mm which is equivalent to 9 layers of cable. Type 2 shown in Fig. 4, was formed by untwisting the Type 3 coil. The calculated multipole components in these three coils are shown in Table 2. Each value was found by Fourier analysis of the integrated azimuthal fields along a circle at a radius of 3.0 cm from the axis on a vertical plane at the longitudinal center of the coil.

Table 2 Comparison with multipole components of the coils without yoke

		Type 1	Type 2	Type 3
Reference radius	cm	3.0	3.0	3.0
Dipole component	Gauss	27100	27400	27900
Sextupole component	Gauss	50.9	60.1	60.9
Decapole component	Gauss	7.14	9.30	9.38
Ratio of Sext. comp.	%	0.188	0.220	0.218
Ratio of Deca. comp.	%	0.0263	0.0340	0.0360

Differences of the multipole components between Type 1 coil and Type 2 coils come mainly from slight difference of the coil positions. The end effect of Type 2 coil also can be considered, however it seems very small, because the analysis was done at the longitudinal center of the coils. Figure 6 indicates this difference of conductor arrangements in the coil cross section. The conductors of Type 1 are arranged along circular arcs, but in the actual magnet, the superconducting cables are placed in rectangular grooves. As for height of conductors, it will be compressed and becomes lower. Accordingly, the coil position in azimuthal direction is not perfect. The only difference between Type 2 and Type 3 is from helicity. Then we can not see the large difference in multipole components between Type 2 and Type 3 using azimuthal field expansion.

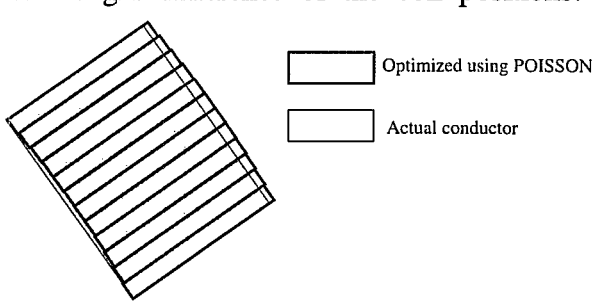

Fig. 6 Coil positions

4. Multipole expansion of the field in Cartesian coordinate

As mentioned above, as long as attention is paid to the azimuthal component, the

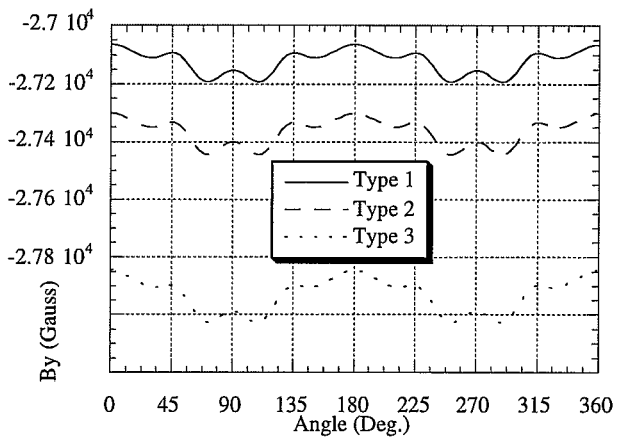

Fig. 7 The vertical component in the coils

effect due to helical structure is very small. Are there any effects to the multipole component? Let us now attempt to extend the analysis into Cartesian coordinates. In many cases, Cartesian coordinates are more convenient than cylindrical coordinates for tracking calculations. Can we just use multipole coefficients obtained from the cylindrical coordinates in the Cartesian coordinates? Is it enough to see only B_θ component, for designing the Snake magnets? Figure 7 shows the vertical field, Y component in Cartesian coordinates, on the circle of 3.0 cm radius at the longitudinal centers of the three types of coils described above. The amplitude of Type 2 is almost same as Type 1, but the amplitude of Type 3 is even larger than others. This can be considered as the effect of helicity. The multipole components calculated using these vertical components are shown in Table 3. The sextupole component of Type 3 obtained from the vertical component, in Table 3, is quite larger than that from the azimuthal component, in Table 2. To estimate precisely the effect due to helical structure on the orbit and the motion of the spin, magnet optimization using only azimuthal fields is not enough.

Table 3 Comparison with multipole components of the coils without yoke using vertical component

		Type 1	Type 2	Type 3
Reference radius	cm	3.0	3.0	3.0
Dipole component	Gauss	27100	27400	27900
Sextupole component	Gauss	50.8	58.1	80.4
Decapole component	Gauss	7.14	9.04	9.14
Ratio of Sext. comp.	%	0.188	0.212	0.288
Ratio of Deca. comp.	%	0.0263	0.0330	0.0327

5. The effect of helical structure on the sextupole component

Let us consider the effect of helical structure on the sextupole component. As a beginning, we will confirm that the multipole coefficients in the cylindrical coordinates can be converted into the Cartesian coordinates, when there are no magnetic field components in the axial direction. Then we will consider the helical magnets.

5.1 In case of straight magnet, 2D, structure.

In cylindrical coordinates, assuming no skew components, the field can be expanded as the following series.

$$B_r = B_0 \sum_0 \left(\frac{r}{r_0}\right)^n b_n \sin(n+1)\theta \qquad (1)$$

$$B_\theta = B_0 \sum_0 \left(\frac{r}{r_0}\right)^n b_n \cos(n+1)\theta \qquad (2)$$

Then, measured or calculated magnetic fields along a circular arc are expanded as the Furrier series, and the multipole components expressed as,

Dipole component	$n=0$	$B_0 b_0$
Quadrupole component	$n=1$	$B_0\left(\frac{r}{r_0}\right)b_1$
Sextupole component	$n=2$	$B_0\left(\frac{r}{r_0}\right)^2 b_2$

To convert these into Cartesian coordinate series,

$$B_x = B_r \cos\theta - B_\theta \sin\theta \qquad (3)$$

$$B_y = B_r \sin\theta + B_\theta \cos\theta \qquad (4)$$

are substituted, which yields the following expressions.

$$B_x = B_0 \sum_0 \left(\frac{r}{r_0}\right)^n \left[b_n \sin(n+1)\theta \cdot \cos\theta - b_n \cos(n+1)\theta \cdot \sin\theta\right]$$
$$= B_0 \sum_0 \left(\frac{r}{r_0}\right)^n b_n \sin n\theta \qquad (5)$$

$$B_y = B_0 \sum_0 \left(\frac{r}{r_0}\right)^n \left[b_n \sin(n+1)\theta \cdot \sin\theta + b_n \cos(n+1)\theta \cdot \cos\theta\right]$$
$$= B_0 \sum_0 \left(\frac{r}{r_0}\right)^n b_n \cos n\theta \qquad (6)$$

In other words, the same coefficients are provided in both coordinate systems.

5.2 In case of helical magnet, 3D, structure.

The expressions for the field of a helical magnet are given by W. Fisher [2]. We use these expressions ignoring skew components.

$$B_r = B_0 \sum_0 f_n I'_{n+1}((n+1)kr)\tilde{b}_n \sin(n+1)\theta \qquad (7)$$

$$B_\theta = \frac{1}{kr} B_0 \sum_0 f_n I_{n+1}((n+1)kr)\tilde{b}_n \cos(n+1)\theta \qquad (8)$$

$$B_s = -B_0 \sum_0 f_n I_{n+1}((n+1)kr)\tilde{b}_n \cos(n+1)\theta \qquad (9)$$

Where,

$$f_n = \frac{2^{n+1}(n+1)!}{(n+1)^{n+1}} \frac{1}{r_0^n k^n} \qquad (10)$$

I is the modified Bessel function.

Again, measured or calculated azimuthal fields along a circular arc are expanded as the Furrier series, and the multipole components are expressed as,

Dipole component	$n = 0$	$B_0 \frac{2}{rk} I_1(kr)\tilde{b}_0$
Quadrupole component	$n = 1$	$B_0 \frac{2}{rr_0 k^2} I_2(2kr)\tilde{b}_1$

Sextupole component $\quad n=2 \quad B_0 \frac{16}{9rr_0^2k^3} I_3(3kr)\tilde{b}_2$

Using (3) (4), the above series are converted in Cartesian coordinates,

$$B_x = B_0 \sum_0 f_n \tilde{b}_n \left[I'_{n+1}((n+1)kr)\sin(n+1)\theta \cdot \cos\theta - \frac{I_{n+1}((n+1)kr)}{kr}\cos(n+1)\theta \cdot \sin\theta \right] \qquad (11)$$

$$B_y = B_0 \sum_0 f_n \tilde{b}_n \left[I'_{n+1}((n+1)kr)\sin(n+1)\theta \cdot \sin\theta + \frac{I_{n+1}((n+1)kr)}{kr}\cos(n+1)\theta \cdot \cos\theta \right] \qquad (12)$$

Here, we assume that the helical dipole magnet is optimized only using B_θ components. As a result, $b_n = 0$ for $n > 0$. So, these expressions can be transformed into,

$$B_x = B_0 \tilde{b}_0 \left[I'_1(kr) - \frac{I_1(kr)}{kr} \right] \sin 2\theta \qquad (13)$$

$$B_y = B_0 \tilde{b}_0 \left[\left(I'_1(kr) + \frac{I_1(kr)}{kr} \right) - \left(I'_1(kr) - \frac{I_1(kr)}{kr} \right) \cos 2\theta \right] \qquad (14)$$

The above expression shows that the B_x component consists of the sextupole terms. Also the B_y component is expressed as a sum of the dipole and sextupole terms. Accordingly, when the magnet is optimized using Furrier expansion of only B_θ, it has to have the sextupole component in Cartesian coordinate. Let us set up a helical pitch with 240 cm, and define functions S and D as

$$k = \frac{2\pi}{240}$$

$$D(r) = \left(I'_1(kr) + \frac{I_1(kr)}{kr} \right) \qquad (15)$$

$$S(r) = \left(I'_1(kr) - \frac{I_1(kr)}{kr} \right) \qquad (16)$$

Functions D and S vary as in Figs 8 and 9.

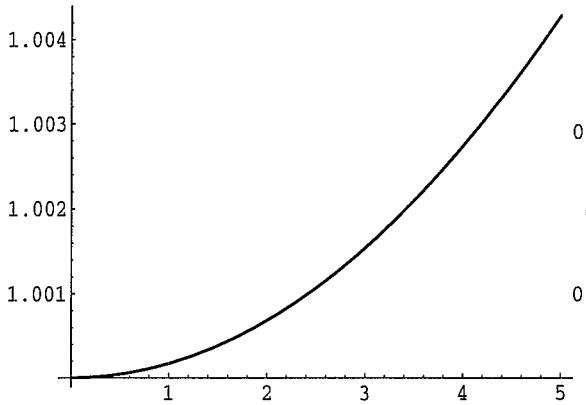

Fig. 8 Function *Dr*. Horizontal axis shows *r*.

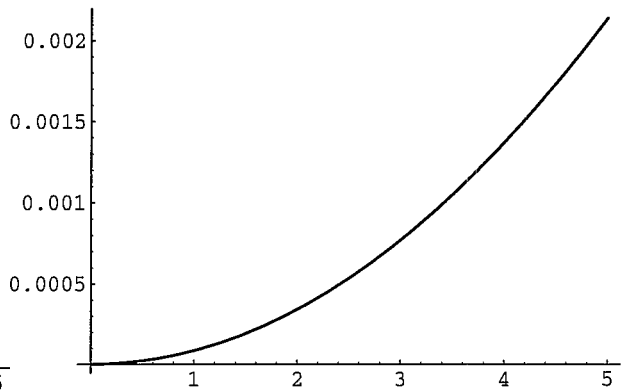

Fig. 9 Function *Sr*. Horizontal axis shows *r*.

The ratio of the sextupole component to the dipole component is 0.0771 % at $r = 3.0$ cm. This value is almost equivalent to a difference between the sextupole components of Type 3 in Table 2 and that in Table 3.

6. The optimization method for 2D analysis.

Seeing only azimuthal component, the difference between Type 2 and Type 3 can be almost ignored as shown in Table 2. In other words, as long as only the coefficients from B_θ components are considered, the optimization by 2D calculation will be good enough. From the beam optical point of view, however, the uniformity required by dipole magnets means the uniformity of the transverse field components. Accordingly, it is important to consider B_y component. As shown in Table 3, the sextupole component, which is caused by the b_0 coefficient, increases. Of course, there are effects caused by higher order coefficients, $n = 1, 2, 3, \cdots$, but these terms can be ignored because the b_0 term is dominant in the Snake magnet. It will be effective to set b_2 as offsetting the effect of being helical due to b_0, when optimization is done by 2D magnetic field calculations. Then, it should be inspected finally by the 3D calculation.

7. The expected multipole components in the actual magnet configuration

The multipole components in the actual magnet configuration, which consists of Type 3 coil and the iron yoke, are calculated. These results are shown in Table 3. The sextupole component changes by 0.4 % due to saturation of the yoke. The sextupole components calculated from the B_y components are from 0.07 % to 0.08 % larger than those calculated from B_θ, and these differences agree with what was described above. So, it is

necessary to confirm that the sextupole components can be optimized by changing the ratio of the electric current in the conductors.

Table 3 The expected multipole components in the actual helical magnets

Field strength		High	Low	Very low
Reference radius	cm	3.0	3.0	3.0
Dipole component	Gauss	41400	11800	1180
Analysis from B_θ				
Sextupole component	Gauss	50.0	59.2	5.90
Decapole component	Gauss	4.70	25.8	2.61
Ratio of Sext. comp.	%	0.121	0.502	0.500
Ratio of Deca. comp.	%	0.0114	0.219	0.221
Analysis from B_y				
Sextupole component	Gauss	79.2	68.7	6.83
Decapole component	Gauss	6.50	27.0	2.63
Ratio of Sext. comp.	%	0.191	0.582	0.579
Ratio of Deca. comp.	%	0.0157	0.229	0.223

8. Conclusion

The magnetic fields in the straight coil, which was optimized using POISSON, were analyzed by TOSCA, and the reliability of TOSCA was confirmed. Then the differences between the coil cross section optimized by POISSON and the cross section being actually fabricated are compared. And, it was shown that the sextupole component derived from the vertical component shows the effect of helicity, but the same component calculated from the azimuthal component does not indicate the obvious effect. Using 2D analysis, to minimize the sextupole component in the vertical field in the helical structure, the predicted sextupole component should be offset. Yet it is important to do 3D analysis finally. In the end, the multipole components in the actual magnet configuration were predicted.

9. Acknowledgment

I wish to thank F. Mariam for useful discussions and reading this manuscript, also grateful to G. Morgan, R. Gupta and E. Willen for information about the Snake magnet. Almost this work had been presented at RHIC Spin Accelerator Seminar, Sept. 1996 RIKEN,

and this note owes much to the thoughtful comments at the seminar.

References

[1] R. Gupta private, communication.

[2] W. Fisher (AGS/RHIC/SN No. 32)